**Gulf of Mexico Hydrate Mapping and Interpretation Analysis**

Phase-II, Project Area 2.3 Report

Aditya Kumar, Alexey Portnov, Ann Cook

November 3, 2023

This report satisfies Mapping and Prospect Identification within Project Area 2.3 for the Bureau of Ocean Energy Management (BOEM) award Gulf of Mexico Gas Hydrate Mapping and Interpretation Analysis, which is Deliverable/Milestone 5.

## Table of Contents



*Table 1. List of required deliverables and figures.*

| Sr. | Deliverable | Figure # |
|---|---|---|
| 1 | A map showing the spatial distribution of BSRs within Project Area 2.3 | 2 |
| 2 | Regional seismic cross sections showing the base of gas hydrate stability. | 4-9, 13 -14, 16-19, 21-22 |
| 3 | RMS amplitude maps that correlate with the identified BSR zones | 3, 12, 15, 20 |
| 4 | Correlation of well logs and seismic data | 6, 9 |

# 1 Study Area

Project Area 2.3 covers ~5,450 $km^2$ and includes the eastern part of the Green Canyon protraction area, a small part of western Atwater Valley, the southwestern corner of Mississippi Canyon, and the southeastern corner of Ewing Bank (as illustrated in Figure 1a). The water depth within this area varies from 120 to 1850 m (as shown in Figure 1b). Areas with a water depth less than 600 m lie outside the methane hydrate stability zone and are not included in the assessment (Figure 2).

For Project Area 2.3, we used ten seismic surveys available at the National Archive of Marine Seismic Surveys (NAMSS; Triezenberg et al., 2016) database (Figure 1a). These surveys completely cover Project Area 2.3. The seismic surveys used for this study are shown in Table 2.

In Project Area 2.3, we have identified a total of six bottom-simulating reflections (BSRs) which were categorized into four distinct zones (Figure 2). Three of the six BSRs were previously identified by BOEM (Shedd et al., 2012); BSRs previously identified by BOEM are shown in Figure 2. All BSRs identified in this study occur over salt structures as observed in other regions of Gulf of Mexico (Portnov and Cook, 2020, 2019; Skopec et al., 2021).

Several wells have been drilled within Project Area 2.3 (Figure 2). The well log data were acquired from the Bureau of Safety and Environmental Enforcement (BSEE) online database. In this report we show three wells in Zone-1 (Figure 3). Zone-2 and Zone-4 do not have wells near the BSRs and wells near Zone-3 do not have log data in the near seafloor sediments within and close to the hydrate stability zone.

Thermogenic gas hydrates were recovered in piston cores at one location on the edge of Project Area 2.3 (Sassen et al., 2001) (Figure 2). This location does not coincide with any identified BSR either in this study or with the BSRs previously identified by BOEM (Figure 2).

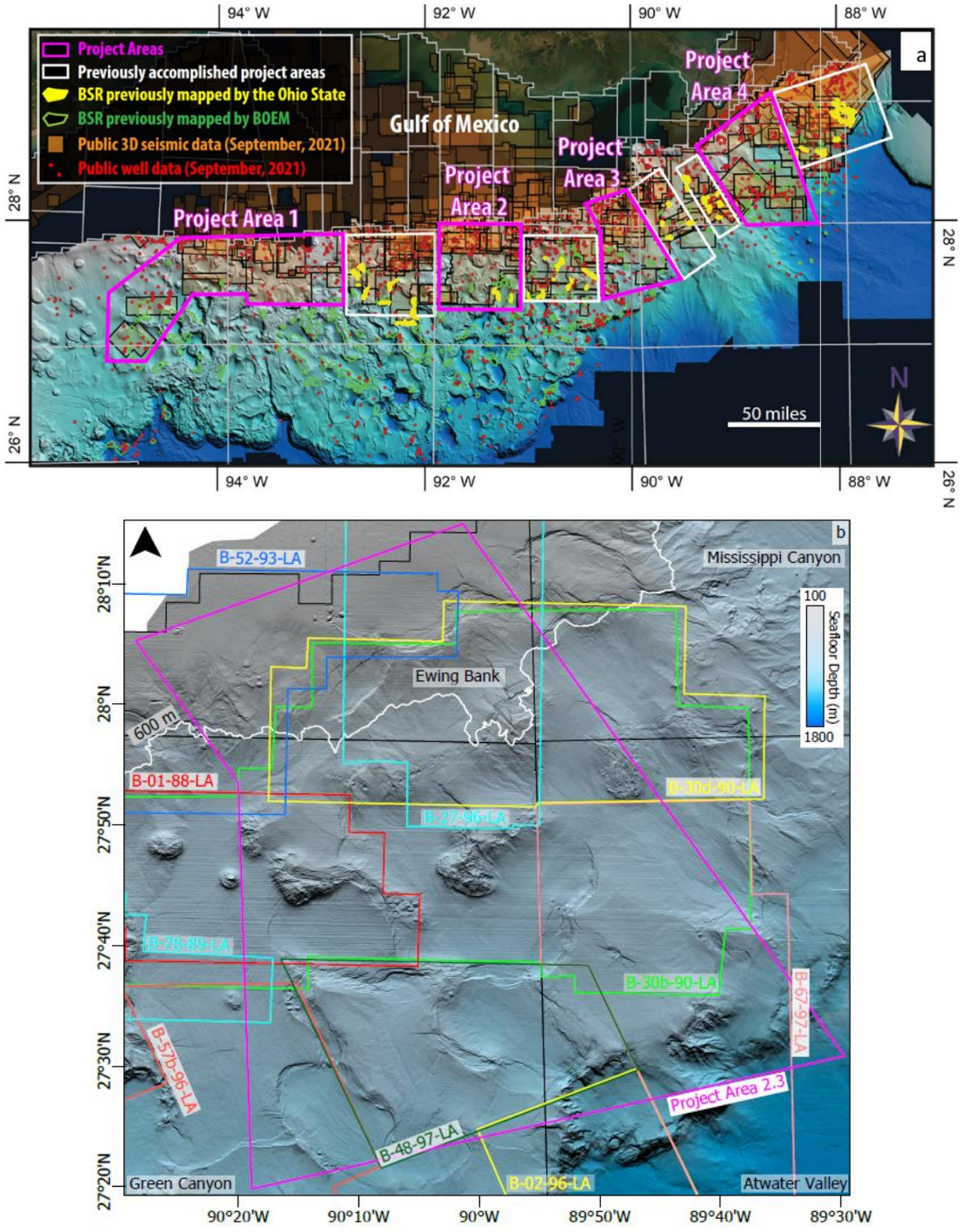


*Figure 1: a) A regional bathymetry map of the northern Gulf of Mexico (bathymetry from Kramer and Shedd, 2017) showing Project Areas of Phase 1 (white squares) and Phase 2 (pink squares). B) Project Area 2.3 and the outline of each seismic survey used in this report (Table 2).*

| | Survey name/BOEM identifier | Year | Area of seismic survey ($km^2$) | Frequency Range (Hz) | Survey quality | Bin size (m) | Projection |
|---|---|---|---|---|---|---|---|
| **1** | B-01-88- LA/L88-001 | 1988 | 1100 | 5-80 | Poor | 40×25 | NAD27 Louisiana State Planes, Southern Zone, US feet |
| **2** | B-78-89- LA/L89-078 | 1989 | 1740 | 8-90 | Poor | 26.6×26.6 | 15N NAD 1927, feet |
| **3** | B-57b-96- LA/L96-57b | 1996 | 1450 | 5-80 | Fair | 20×12.5 | 15N NAD 1927, feet |
| **4** | B-52-93- LA/L93-052 | 1993 | 2050 | 5-80 | Poor | 20×12.5 | NAD27 Louisiana State Planes, Southern Zone, US feet |
| **5** | B-27-96- LA/L96-027 | 1996 | 1750 | 8-80 | Poor-Fair | 20×12.5 | 15N NAD 1927, feet |
| **6** | B-48-97- LA/L97-048 | 1997 | 1000 | 5-80 | Poor-Fair | 20×12.5 | 15N NAD 1927, feet |
| **7** | B-30d-90- LA/L90-30d | 1990 | 1720 | 5-80 | Poor | 26.6×26.6 | 15N NAD 1927, feet |
| **8** | B-30b-90- LA/L94-025 | 1990 | 4150 | 5-85 | Poor-Fair | 20×25 | 15N NAD 1927, feet |
| **9** | B-02-96- LA/L96-002 | 1996 | 600 | 5-90 | Fair-Good | 20×12.5 | 16N NAD 1927, feet |
| **10** | B-67-97- LA/L97-067 | 1997 | 1525 | 5-85 | Fair | 20×12.5 | 16N NAD 1927, feet |

*Table 2: The 3D seismic surveys uploaded for initial data quality analyses within Project Area 2.3. Projected coordinate systems: NAD_1927_BLM_Zone_15N [EPSG, 32066], NAD27 Louisiana State Planes, Southern Zone [EPSG, 502034]. The project coordinate system used in Petrel is NAD_1927_BLM_Zone_15N [EPSG, 32066].*

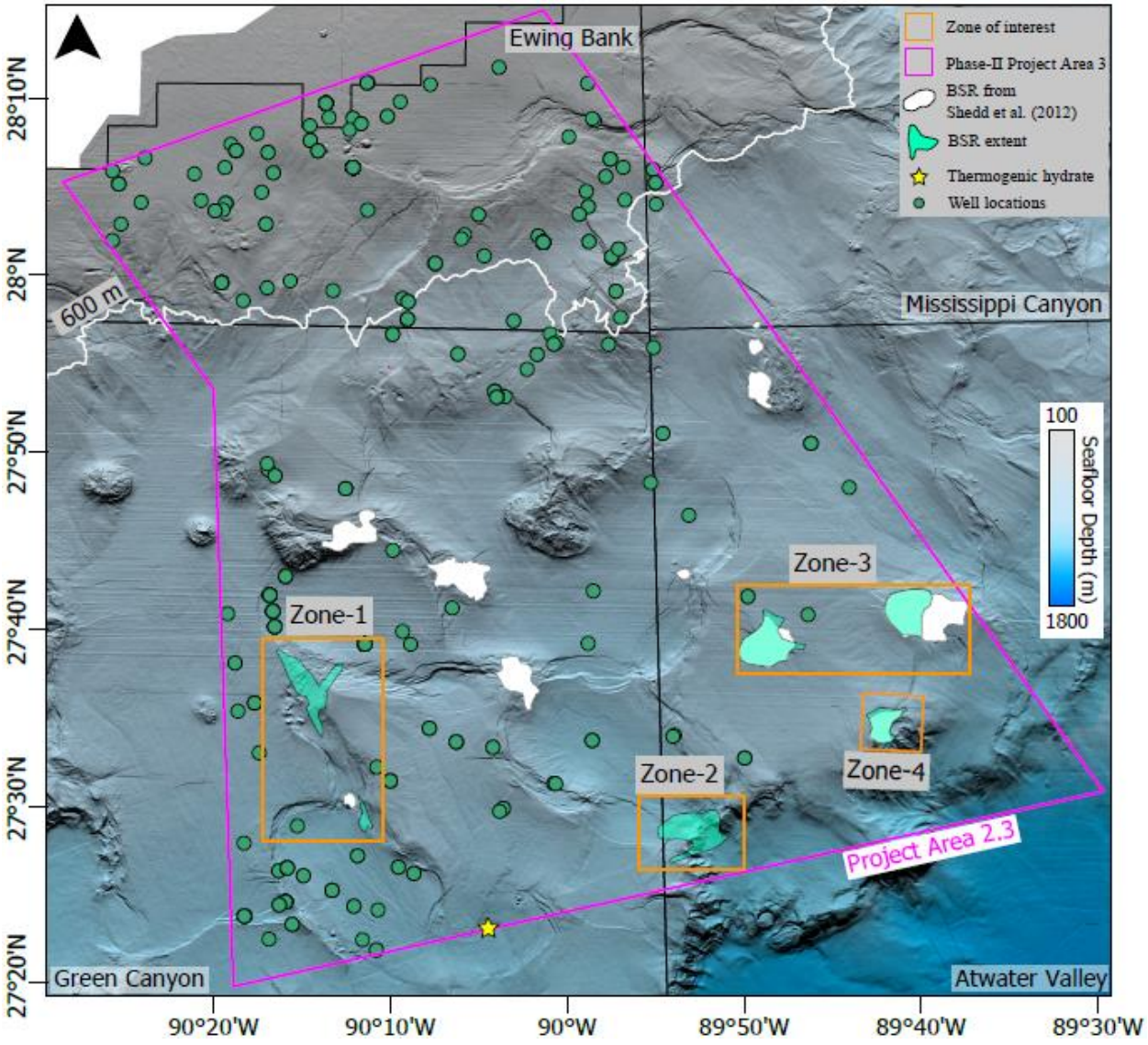


*Figure 2: The bathymetry of Project Area 2.3 from Kramer and Shedd (2017). The white shapes represent the BSRs previously interpreted by BOEM (Shedd et al., 2012). Light green shapes represent the BSRs interpreted in this report. Interpreted BSRs are grouped into four zones shown by the orange rectangles. The white line shows the 600 m water depth contour. The yellow star shows the location of piston cores where thermogenic hydrate was observed by Sassen et al (2001).*

# 2 RMS Mapping

To identify possible BSRs in Project Area 2.3, regional root-mean-square (RMS) amplitude calculations were performed independently within all 3D seismic surveys (Figure 1a). The detailed workflow can be found in the report for Phase 1 Project Area 1. Within this report, we use 100 millisecond (msec) time windows to show the BSR extent on RMS amplitude maps.

Due to heat-conductive shallow salt bodies in this area, the geothermal gradient is highly variable, which significantly perturbs the base of the gas hydrate stability zone. Therefore, RMS amplitude maps are computed within the different time windows below the seafloor. RMS amplitude maps that correlate with the identified BSR zones are shown in Section 4 of this report.

# 3 Classification of BSRs

We classify BSRs into three different types based on their characteristics in the seismic data: continuous BSRs, discontinuous BSRs, and clustered BSRs. Continuous BSRs are continuous, coherent seismic reflections with reversed (trough-leading) polarity that crosscuts primary stratigraphy and is congruent with seafloor morphology (Hillman et al., 2017; Vanneste et al., 2001). Discontinuous BSRs, also referred to as ‘patchy BSRs’, are characterized by segmented and non-coherent lateral reflections that typically align with the seafloor topography (Hillman et al., 2017; Shedd et al., 2012). A third type of BSR is called a clustered BSR, which is characterized as thick, clustered assemblages of high amplitude reflections with its top roughly aligning with the overlying seafloor bathymetry (Portnov et al., 2019). In particular, clustered BSRs occur in the regions with folding or salt tectonics because these regions host multiple anticlinal and domal structures that can trap gas underneath the gas hydrate stability zone (GHSZ). Such BSRs are common in the Gulf of Mexico and warrant special attention because these BSRs may indicate high concentrations of gas hydrate in turbidite sands (Portnov et al., 2019).

# 4 Results in Project Area 2.1

## 4.1 Zone-1

Zone-1 is located in the Green Canyon protraction area (Figure 2). The water depth in this zone varies from 950 to 1300 m. We have identified and mapped two distinct BSR systems within Zone-1 (Figures 2 & 3). Neither of these BSR systems were previously identified by BOEM. These BSRs are identified in seismic volumes B-48-97-LA and B-78-89-LA.

The northern BSR system in Zone-1 covers ~16 $km^2$, while the BSR in the southeastern part is much smaller, covering only a 2.5 $km^2$ area. The depths of the BSRs in this zone range from 180 msec TWT (~150 meters below seafloor (mbsf)) to 390 msec TWT (~350 mbsf) below the seafloor. BSR depth is estimated assuming an average velocity of 1700 m/s in the shallow sediments. Figures 4-9 display the BSRs across Zone-1. The northern BSR is discontinuous while southwestern BSR is continuous. Above the southwestern BSR, we observe a patch of reflections which, in some areas, could be a peak leading reflection (Figures 3, 7 & 8). These reflections often have a relatively strong negative reflection above, however, making the designation 'peak-leading' uncertain. In addition, the extent of this patch is very small and covers only a 0.35 $km^2$ (86 acres) area. In this report, we call these reflections possible peak-leading and have less confidence than peak-leading reflections we have observed in other areas.

There are several wells within Zone-1 (Figures 2 & 3), however none of them penetrate the identified BSRs. The three wells closest to the northern BSR are #608114042100 (2.5 km away), #608114048300 (3.5 km away) and #608114045000 (3.5 km away). The latter two wells are very close to each other and have the same features, therefore, we only used one in our figures. Wells #608114042100 and #608114048300 are shown on the seismic data (Figure 6). The seismic-to-well tie is performed using the velocity function provided by Cook and Sawyer (2015). These wells have ~700 ft thick sand intervals as observed on the gamma ray logs (Figure 6). However, in this area, the rise of a salt diapir has disturbed the shallow sedimentary layers; the sand intervals may have been uplifted with the buoyant salt and now lie near the BSR depth.

The well close to the southeastern BSR (#608114053300) is located nearly 3.5 km away from the BSR. The gamma ray log and one resistivity log from this well are shown on the seismic data

(Figure 9). The gamma ray log does not show any significant change in the lithology in the GHSZ; taken together, the sediment in the GHSZ is likely mud rich turbidites, with very thin (cm scale to 10s of cm scale) sand layers. We analyze the P40H resistivity log and observe an increase in resistivity from 1 ohm-m (background resistivity) to 1.5-3 ohm-m in the shallow sediments above the expected base of GHSZ (Figure 10). However, other propagation resistivity curves (P16H and P28) have more erratic responses in the same interval, with high resistivity spikes. It is therefore difficult to conclude that the observed increase in resistivity in P40H is due to the presence of hydrate, though it might be.

We derive geothermal gradients from the BSR assuming an equilibrium model: 1) heat flow is constant, one-dimensional (vertical), and occurs only through conduction; 2) pore pressure is hydrostatic; 3) pore fluid salinity is 3.5 %; and 4) gas composition is pure methane. We estimate the geothermal gradient in Zone-1 between 30°- 50° C/km.

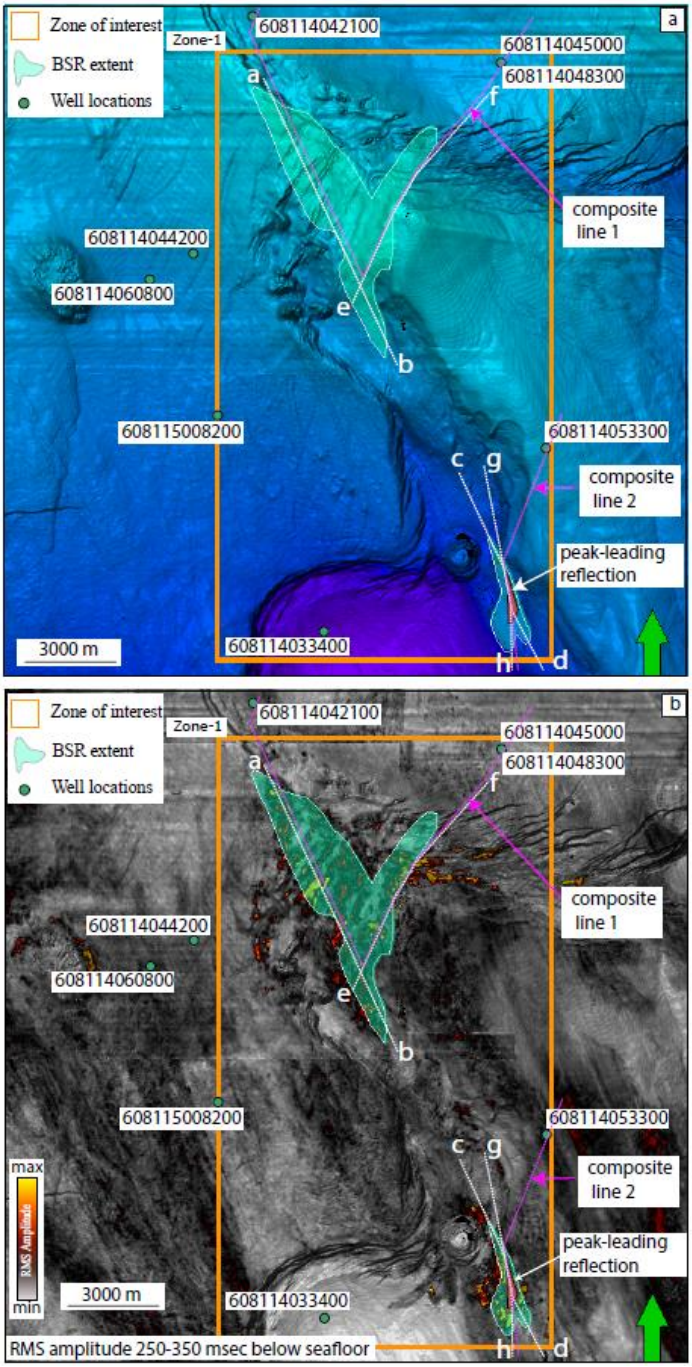


*Figure 3: a) A bathymetry map showing a BSR extent within Zone-1 of Project Area 2.3 (Kramer and Shedd, 2017). The map also shows the wells drilled within or near the Project Area 2.3. A possible peak-leading reflection (red) is observed within the southeastern BSR. b) An RMS amplitude map within 250 - 350 msec window below the seafloor highlights areas with elevated amplitudes corresponding to the BSR zones. White dashed lines show the seismic profile locations in the following figures.*

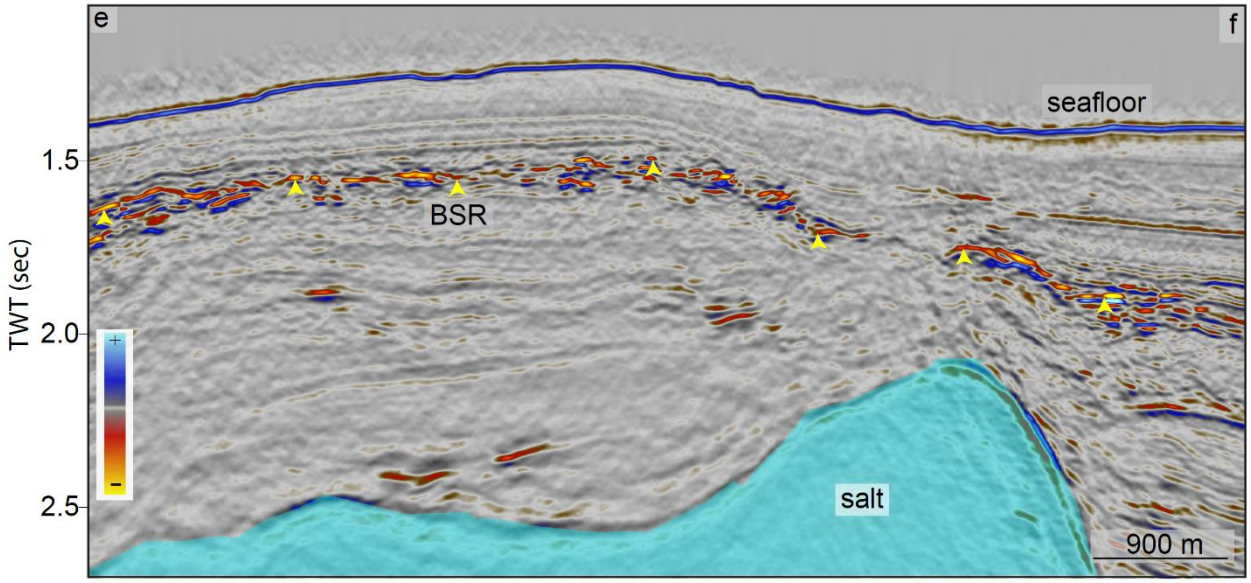


*Figure 4: Seismic profile e-f showing a northwest-southeast cross-section across the northern BSR system of Zone-1. Yellow arrows identify the BSR. The profile location is shown in Figure 3.*

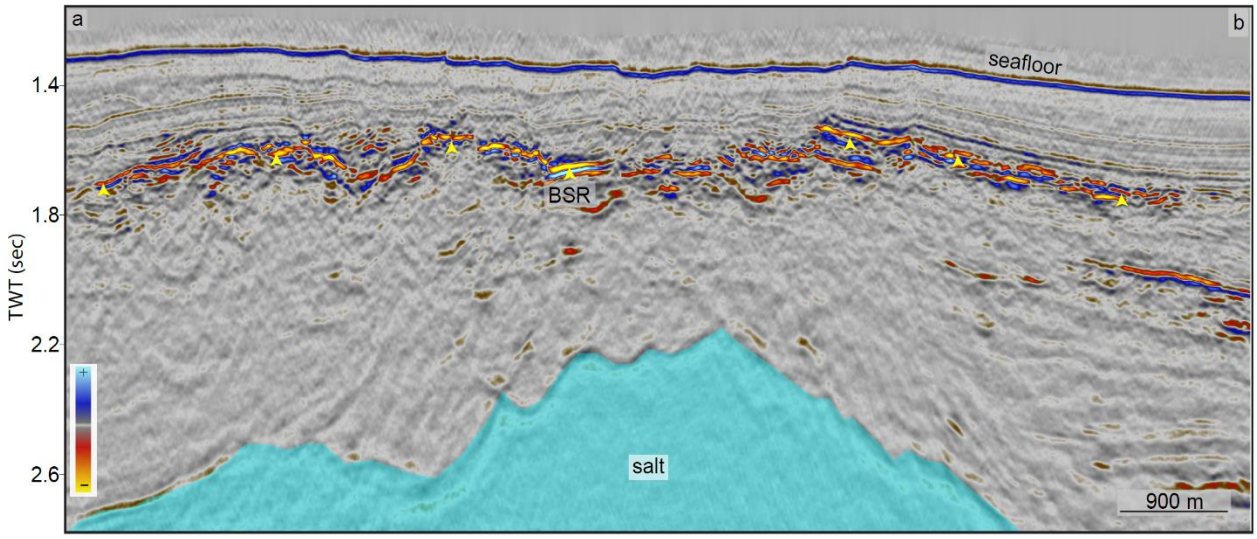


*Figure 5: Seismic profile a-b showing a southwest-northeast cross-section across the northern BSR system of Zone-1. Yellow arrows identify the BSR. The profile location is shown in Figure 3.*

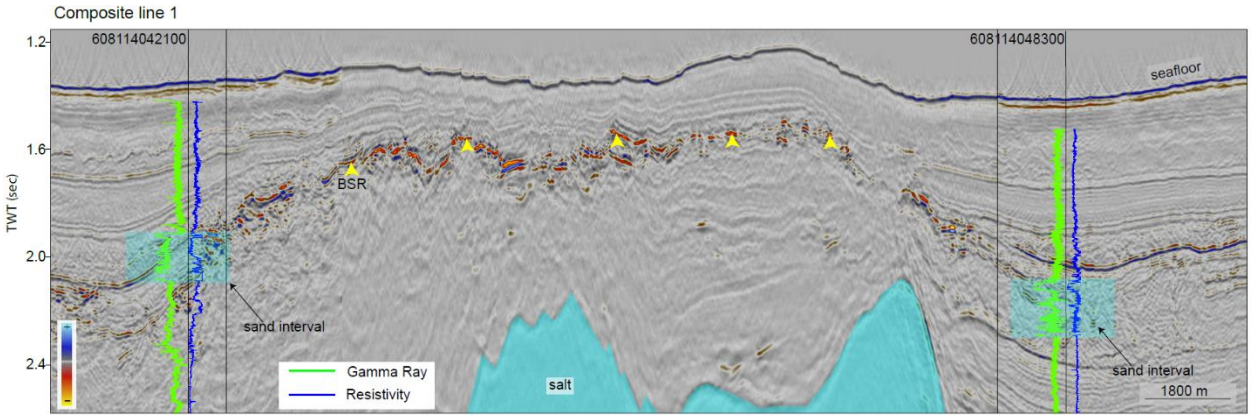


*Figure 6: This is a composite seismic line showing a cross-section across the northern BSR system of Zone-1. The two nearest wells to this BSR are # 608114042100 (2.5 km away) and # 608114048300 (3.5 km away). The gamma ray (green) and resistivity (blue) logs from these wells are projected on the seismic section. Because wells are away from the salt, it is difficult to track the seismic layers above the salt up to the wells, however, there is a chance that the sands may have been pushed up with the rising salt and now coincide with the BSR. The profile location (composite line 1) is shown in Figure 3.*

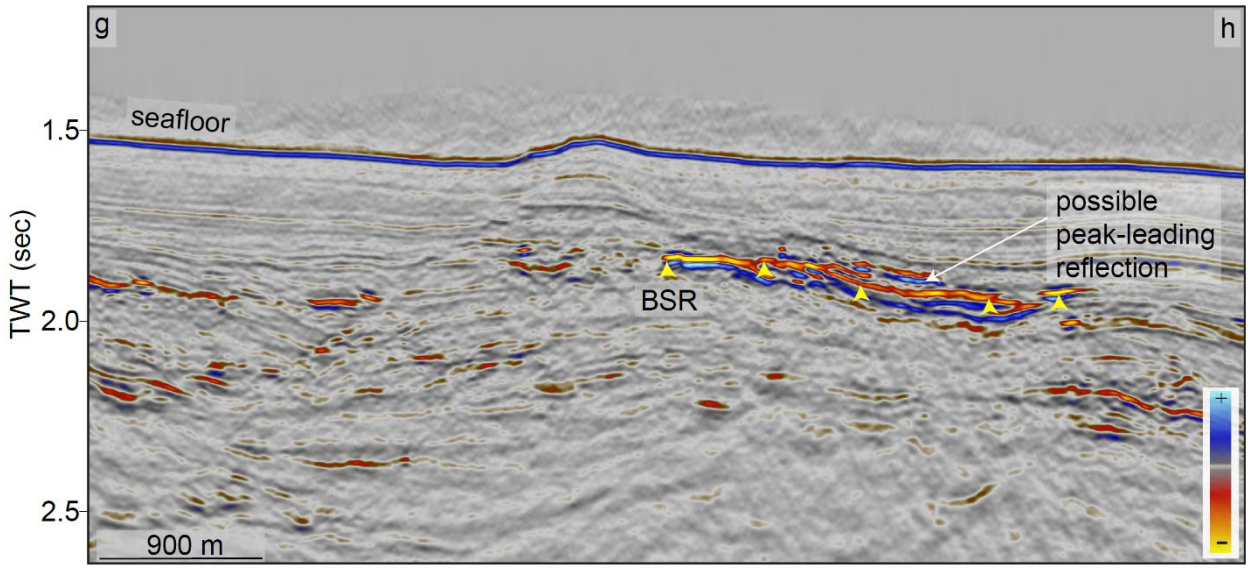


*Figure 7: Seismic profile g-h showing a north-south cross-section across the southeastern BSR system of Zone-1. The BSR is shown by the yellow arrows. A possible peak-leading reflection is also observed across this profile. The profile location is shown in Figure 3.*

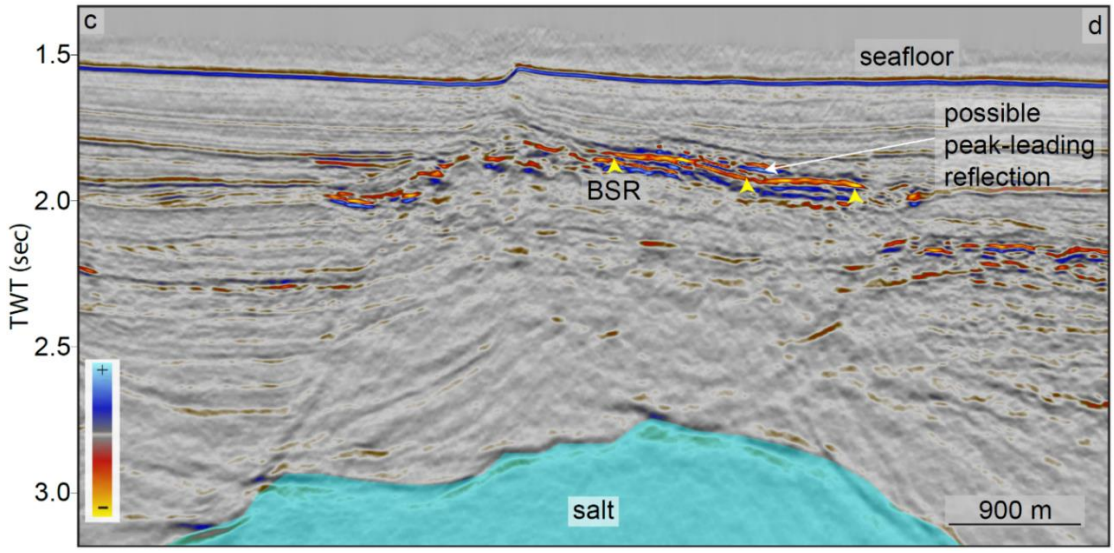


*Figure 8: Seismic profile c-d showing a northwest-southeast cross-section across the southeastern BSR system of Zone-1. The BSR is shown by the yellow arrows. A possible peak-leading reflection is also observed across this profile. The profile location is shown in Figure 3.*

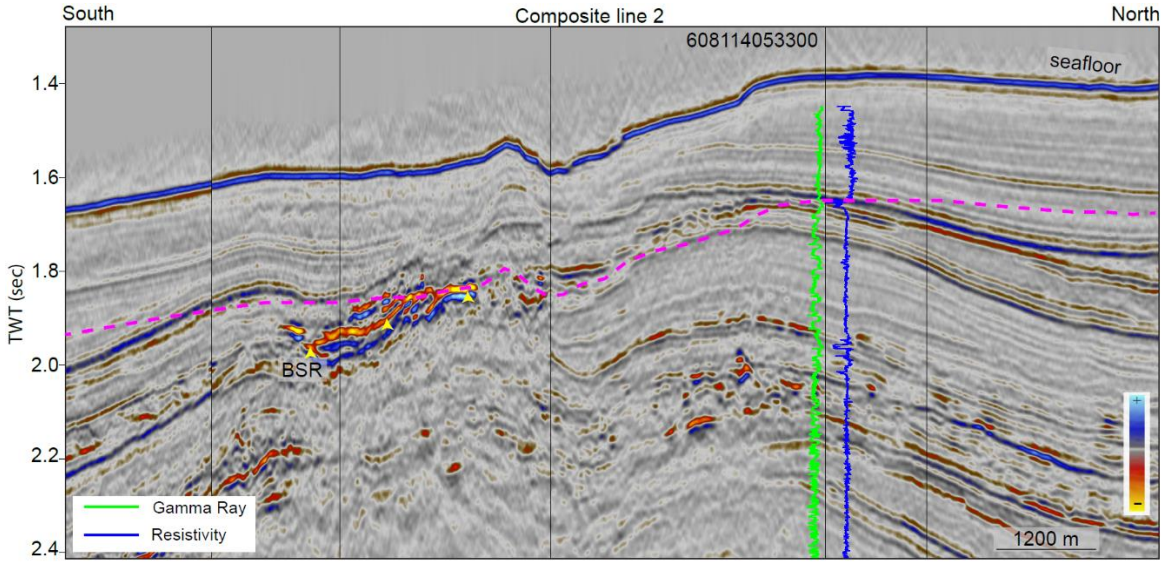


*Figure 9: This is a composite seismic profile showing a cross-section across the southeastern BSR system of Zone-1. The BSR is shown by the yellow arrows. The nearest well to this BSR is API # 608114053300 (3.5 km away). The gamma ray (green) and resistivity (blue) logs from this well are projected on the seismic section. We observe an increase of 0.5-2 ohm-m in resistivity compared to background resistivity (1 ohm-m) indicating the possible presence of hydrate in shallow sediments above the extrapolated BSR indicating approximate base of HSZ. The profile location (composite line 2) is shown in Figure 3.*

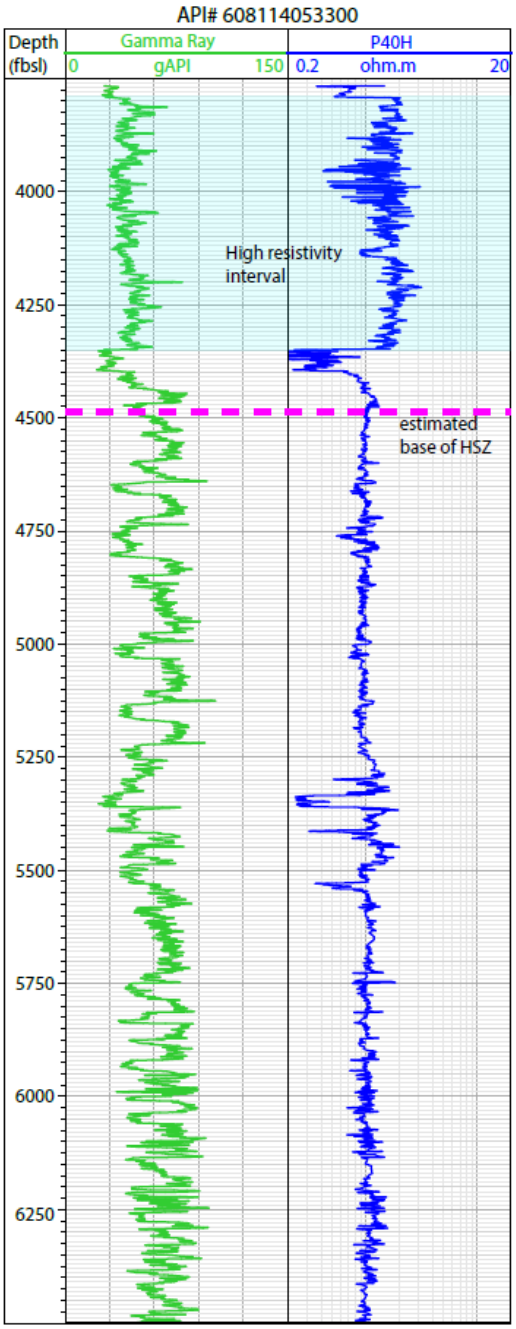


*Figure 10: Gamma ray and resistivity logs from well API# 606114053300. The P40H resistivity log has an increase in resistivity up to 2 ohm-m more than the background resistivity (1 ohm-m), indicating the possible presence of hydrate in this interval. A pink dashed line shows the approximate location of the base of the HSZ assuming geothermal gradient of 30 °C/km and 5°C seafloor temperature.*

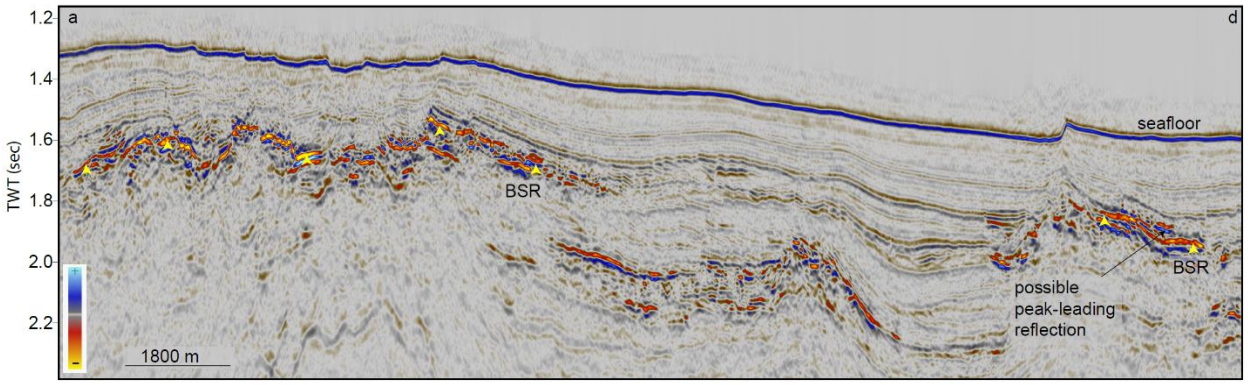


*Figure 11: Seismic profile a-d is a northwest-southeast cross-section showing both of the BSRs in Zone-1. The BSRs are shown by the yellow arrows.*

## 4.2 Zone-2

Zone-2 is within the Atwater Valley protraction area, with water depths ranging from 1200 m to 1475 m. In Zone-2, we have identified only one BSR system, which was not previously mapped by BOEM (Figures 2 & 12). This BSR is identified in seismic volumes B-48-97-LA and B-02-96-LA and it covers an area of 20 $km^2$.

The BSR depths within this single system range from 20 msec to 410 msec TWT beneath the seafloor, corresponding to depths of ~15 m to ~350 m below the seafloor when assuming an average velocity of 1700 m/s. The BSR approaches the seafloor above the salt dome. Shallowing salt changes the geothermal gradient which is likely the cause of the shallow BSR. The seismic profiles in Figures 13 and 14 show this continuous BSR in Zone-2. We observe several northeast-southwest trending faults on the bathymetry within this BSR system (Figure 12a). Selected significant faults extending into and through the GHSZ, are interpreted on the seismic section (Figures 13).

There are no wells near this BSR system.

The estimated geothermal gradient within the BSR area varies between 35–52 °C/km, with the highest geothermal gradient above the salt.

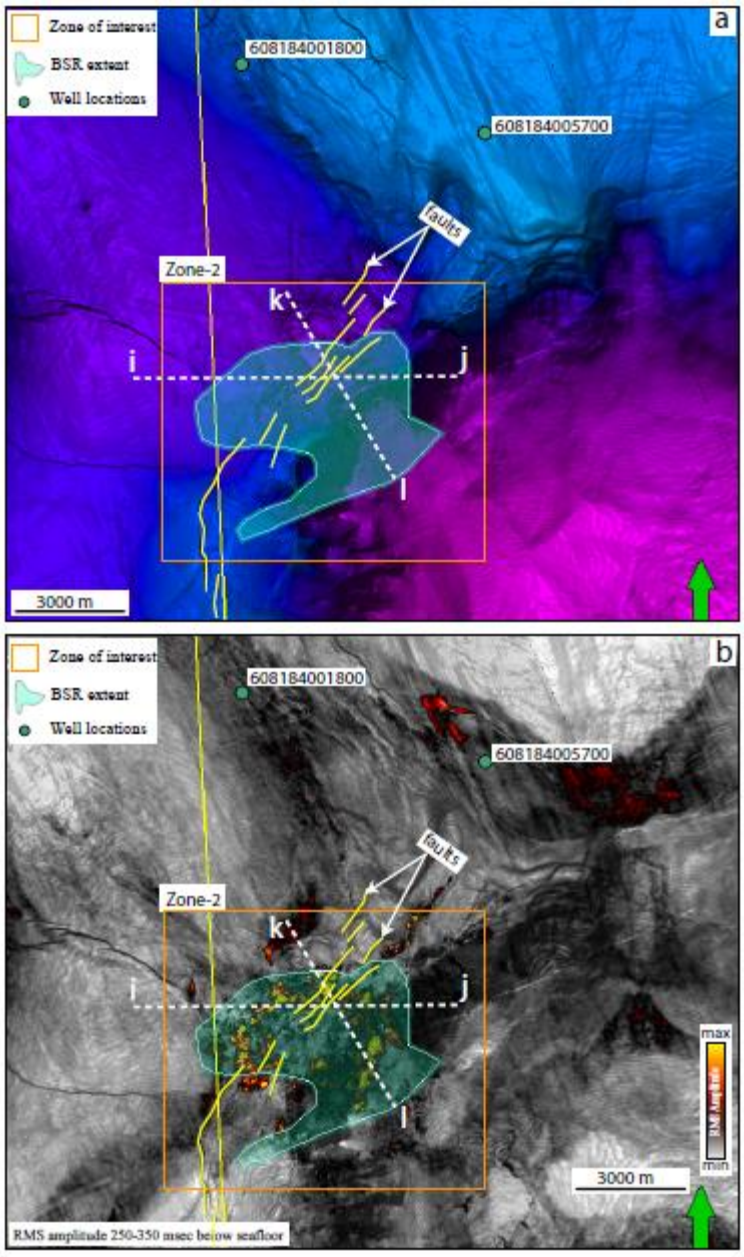


*Figure 12: a) A bathymetry map showing the BSR extent within Zone-2 of Project Area 2.3 (Kramer and Shedd, 2017). White dashed lines show the track of seismic profiles shown in Figures 12 and 13. Solid yellow lines represent the faults. b) An RMS amplitude map within 250 - 350 msec window below the seafloor highlights areas with elevated amplitudes corresponding to the BSR zones. The RMS amplitude map is generated using the seismic volumes B-48-97-LA and B-02-96-LA.*

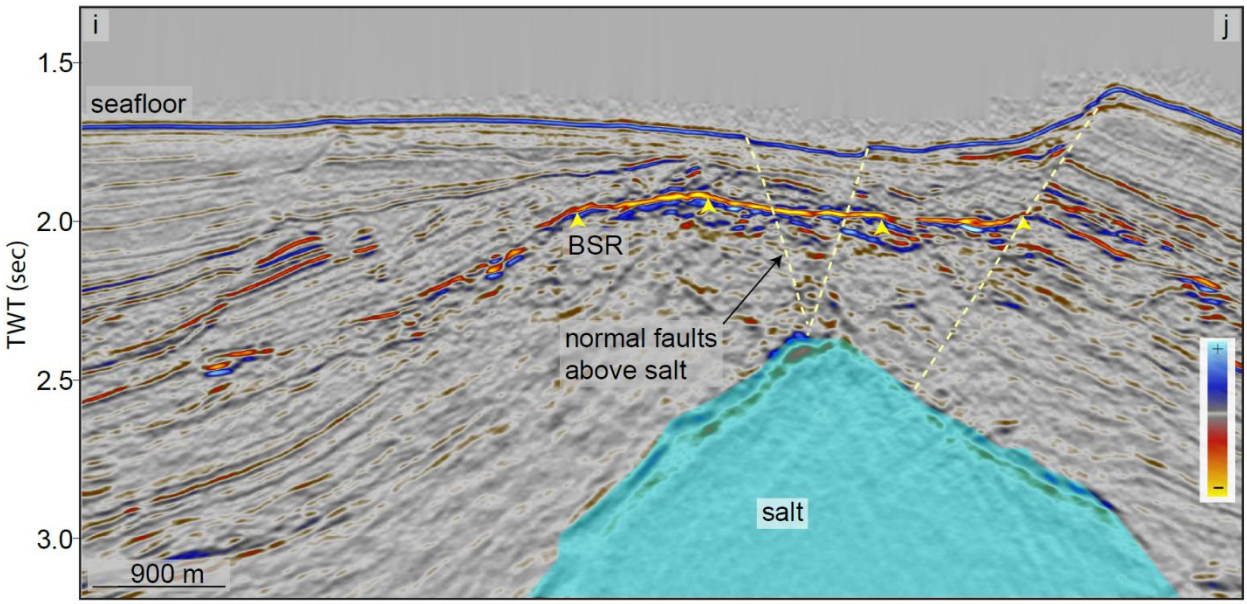


*Figure 13: Seismic profile i-j showing a west-east cross-section across the BSR system in Zone-2. The BSR is shown by the yellow arrows. The profile location is shown in Figure 12a.*

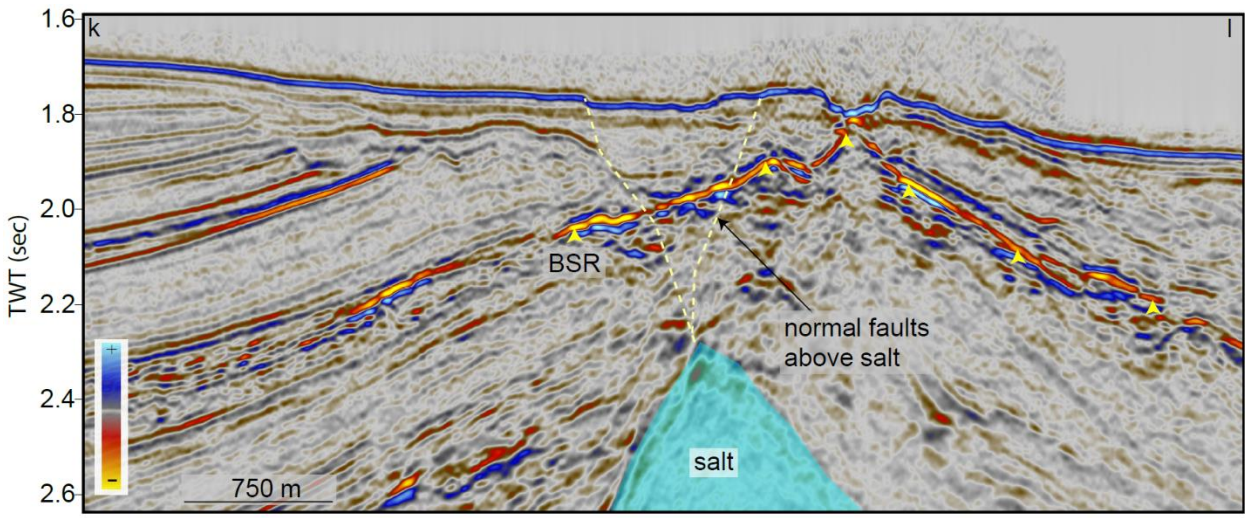


*Figure 14: Seismic profile k-l showing a north-south cross-section across the BSR system in Zone-2. The BSR is shown by the yellow arrows. The profile location is shown in Figure 12a.*

## 4.3 Zone-3

Zone-3 is in the Atwater Valley protraction area, with water depths from 950 m to 1200 m (Figure 2). Two BSR systems, the eastern and western BSR systems, are observed in Zone-3 (Figure 15) in seismic volume B-67-97-LA. These BSRs were previously identified by BOEM, though the mapped areas do vary somewhat between each interpretation (Figure 15). For example, our interpretation of the extent of the eastern BSR in Zone 3 is nearly half the size of the BOEM interpretation. Possibly, this difference in interpretation is the result of BOEM using a newer dataset or several newer datasets that are of better quality and not yet publicly released.

The eastern BSR system in Zone-3 covers an 18 $km^2$ area and is discontinuous (Figures 15, 16, and 17). In the eastern BSR system, the BSR is between 150 to 450 msec below seafloor or 130 to 380 mbsf (Figure 16 and 17). The shallow salt most likely causes the shallow BSR depth due to a local increase in the geothermal gradient above the salt.. The eastern BSR is discontinuous. The estimated geothermal gradient at the eastern BSR ranges between 30 – 60°C/km; the sections of the BSR farthest from the salt have a geothermal gradient of 30 °C/km and intervals above the salt have the highest geothermal gradient.

The western BSR system in Zone 3 is clustered and discontinuous and spans an area of 15 $km^2$ (Figure 15, 18, and 19). The salt is very deep beneath the western BSR system. The western BSR is observed between 600 msec to 800 msec below the seafloor or 510 and 680 mbsf (Figure 18 and 19). Based on the BSR depths, the estimated geothermal gradient in the western BSR area is 20°C/km. There are two wells #608184005000 and #608184000300 located 2.5 and 2 km away from the western BSR system, respectively, but both wells do not have public logging data in shallow interval.

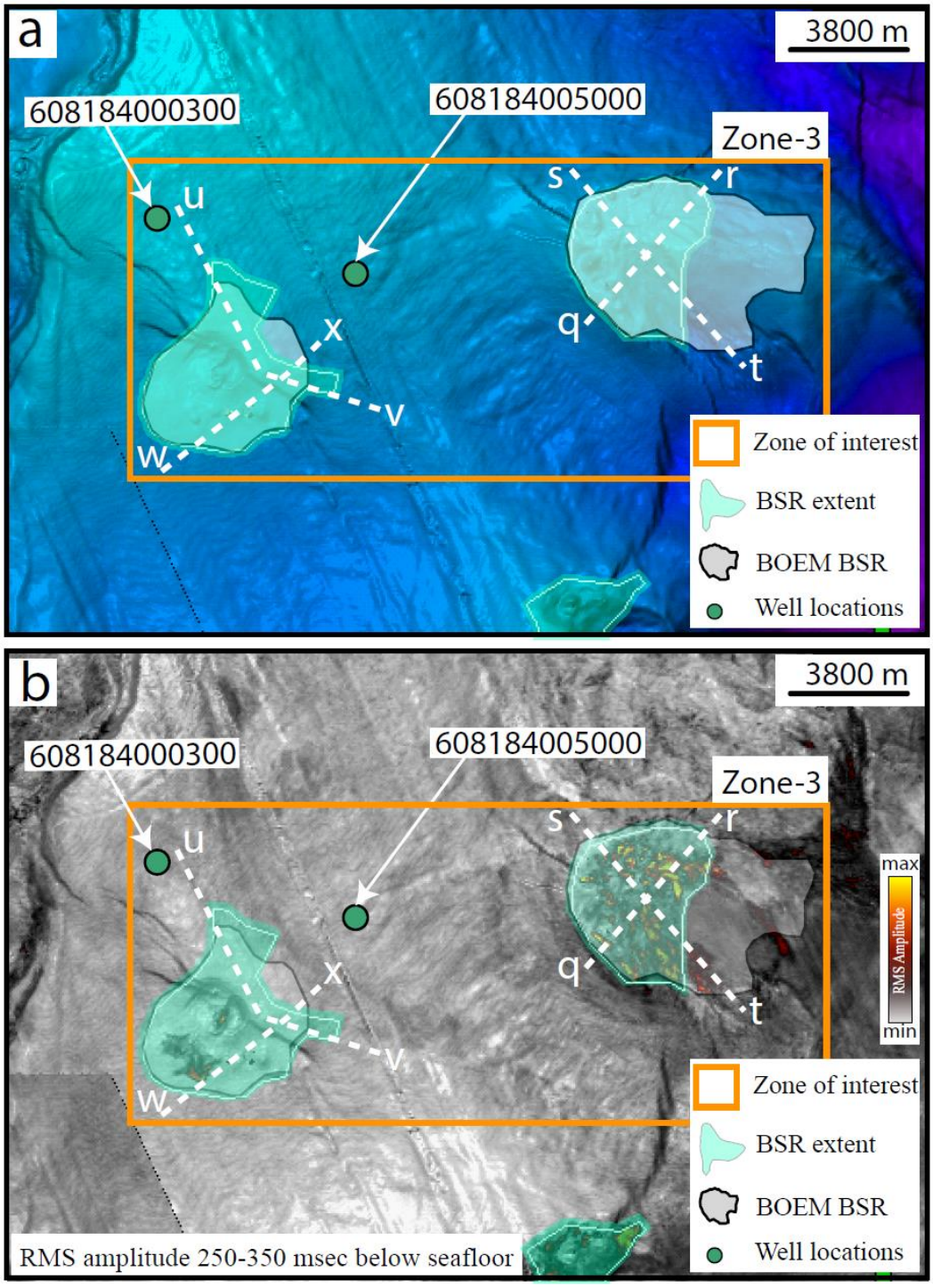


*Figure 15: a) A bathymetry map showing the BSR extent within Zone-3 of Project Area 2.3 (Kramer and Shedd, 2017). White dashed lines show the track of the seismic profiles in the following figures. b) An RMS amplitude map within 250 - 350 msec window below the seafloor highlights areas with elevated amplitudes corresponding to the BSR zones. The RMS amplitude map is generated using the seismic volume B-67-97-LA.*

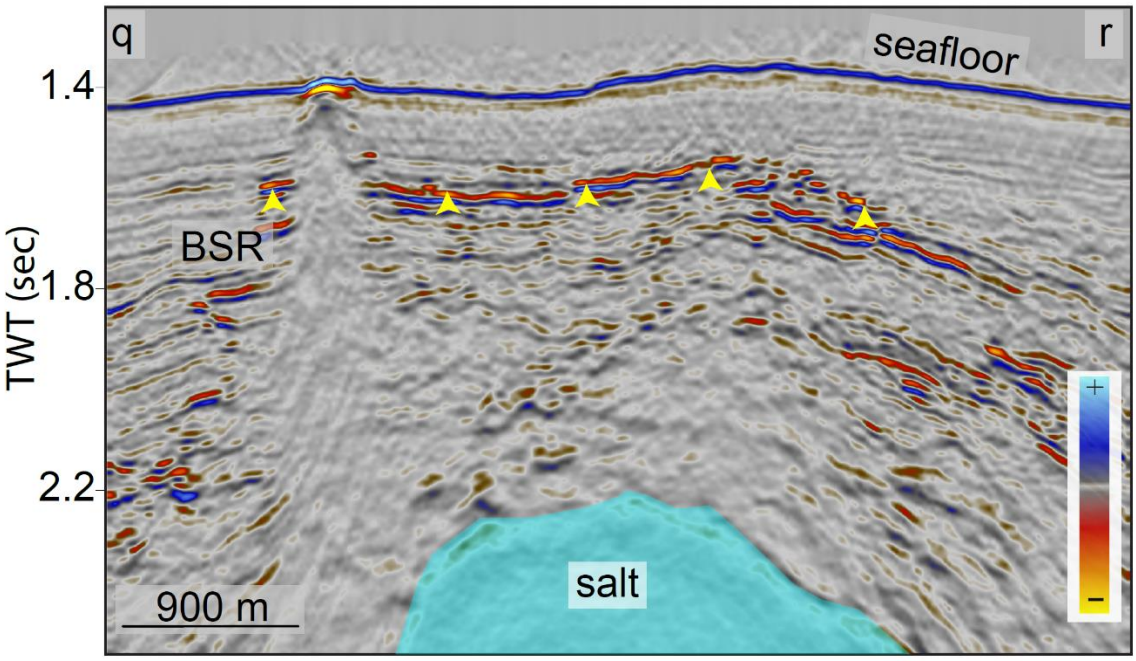


*Figure 16: Seismic profile q-r showing a southwest-northeast cross-section across the eastern BSR system in Zone-3. The BSR is shown by the yellow arrows. The profile location is shown in Figure 15a.*

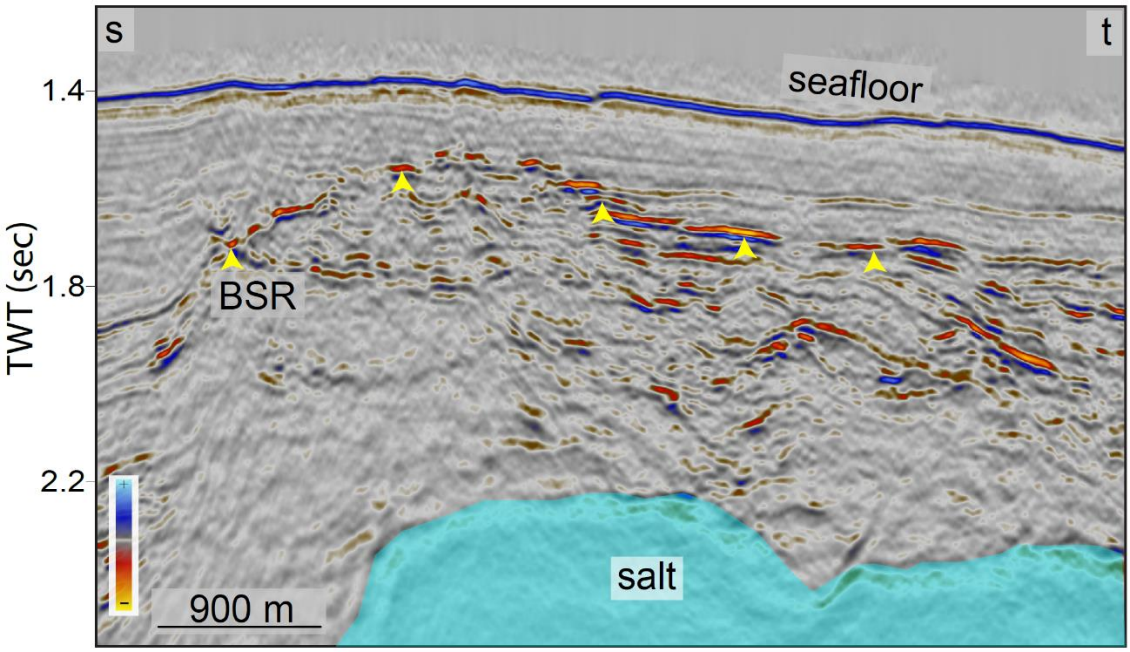


*Figure 17: Seismic profile s-t showing a northwest-southeast cross-section across the eastern BSR system in Zone-3. The BSR is shown by the yellow arrows. The profile location is shown in Figure 15a.*

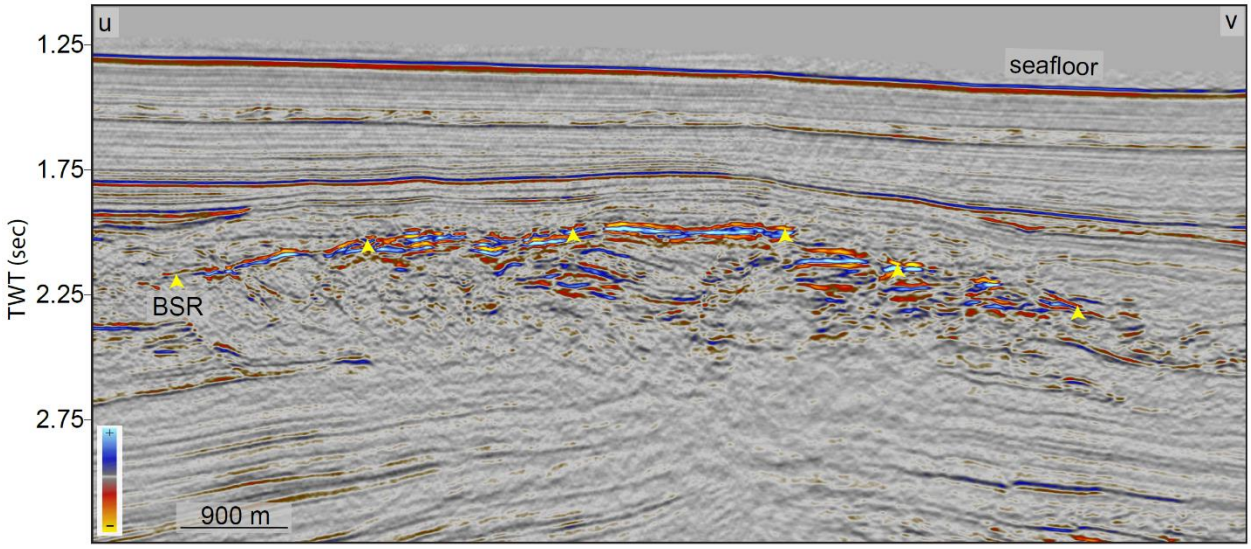


*Figure 18: Seismic profile u-v showing a northwest-southeast cross-section across the western BSR system in Zone-3. The BSR is shown by the yellow arrows. The profile location is shown in Figure 15a.*

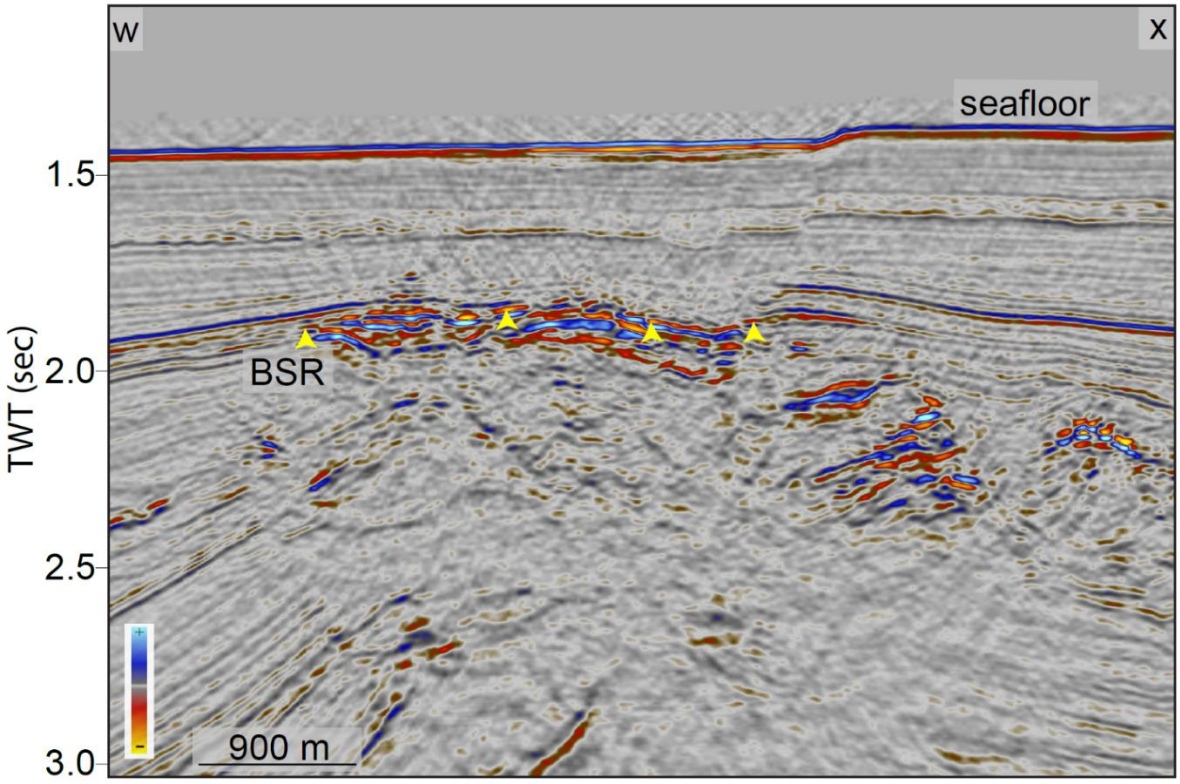


*Figure 19: Seismic profile w-x showing a southwest-northeast cross-section across the western BSR system in Zone-3. The BSR is shown by the yellow arrows. The profile location is shown in Figure 15a.*

## 4.4 Zone-4

Zone-4 is in the Atwater Valley protraction area, with water depths from 1050 m to 1400 m (Figure 2). Only one BSR system has been identified in Zone 4 (Figure 20) in seismic volume B-67-97-LA. This BSR was previously identified by BOEM (Figure 20).

The BSR system in Zone-4 covers an area of 8.5 $km^2$. Figures 21 and 22 show this discontinuous BSR in seismic profiles. This BSR system is located above salt and the depth of the BSR varies from 50 msec to 300 msec TWT below the seafloor, corresponding to depths of 42 to 255 mbsf. Based on the BSR depths, the estimated geothermal gradient in Zone 4 is 40-200 °C/km. To maintain a high geothermal gradient at the shallowest part of the BSR, hot advective fluids are likely flowing up the 500 to 1500 m-wide vent below the shallowest part of the BSR (Figures 20-22). The extent of the vent is indicated by amplitude blanking zone shown with yellow shadings in Figures 21 and 22.

There are no well logs available near Zone-4.

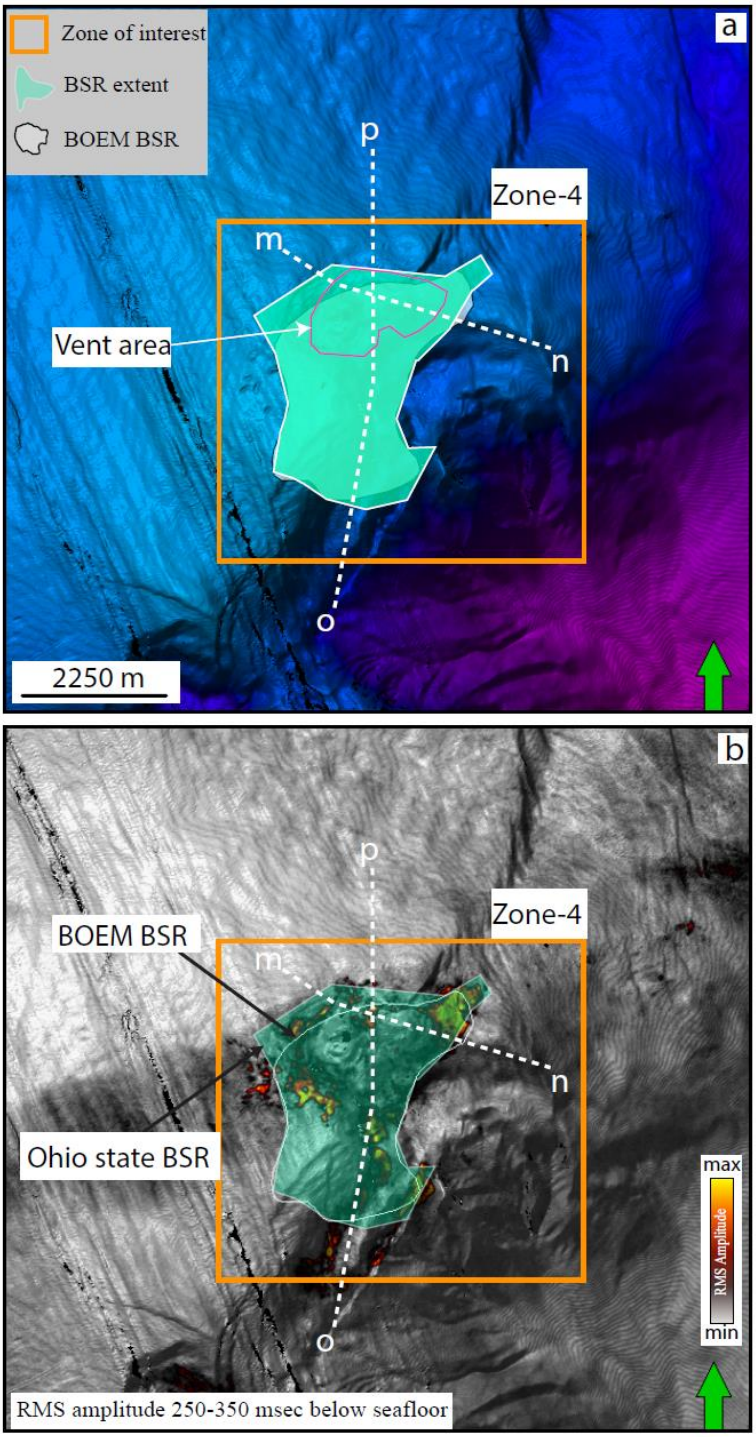


*Figure 20: A bathymetry map* (Kramer and Shedd, 2017) *showing the BSR extent within Zone-4 of Project Area 2.3. White dashed lines show the track of seismic profiles. b) An RMS amplitude map within 250-350 msec window below the seafloor highlights areas with elevated amplitudes corresponding to the BSR zones. The RMS amplitude map is generated using the seismic volume B-67-97-LA.*

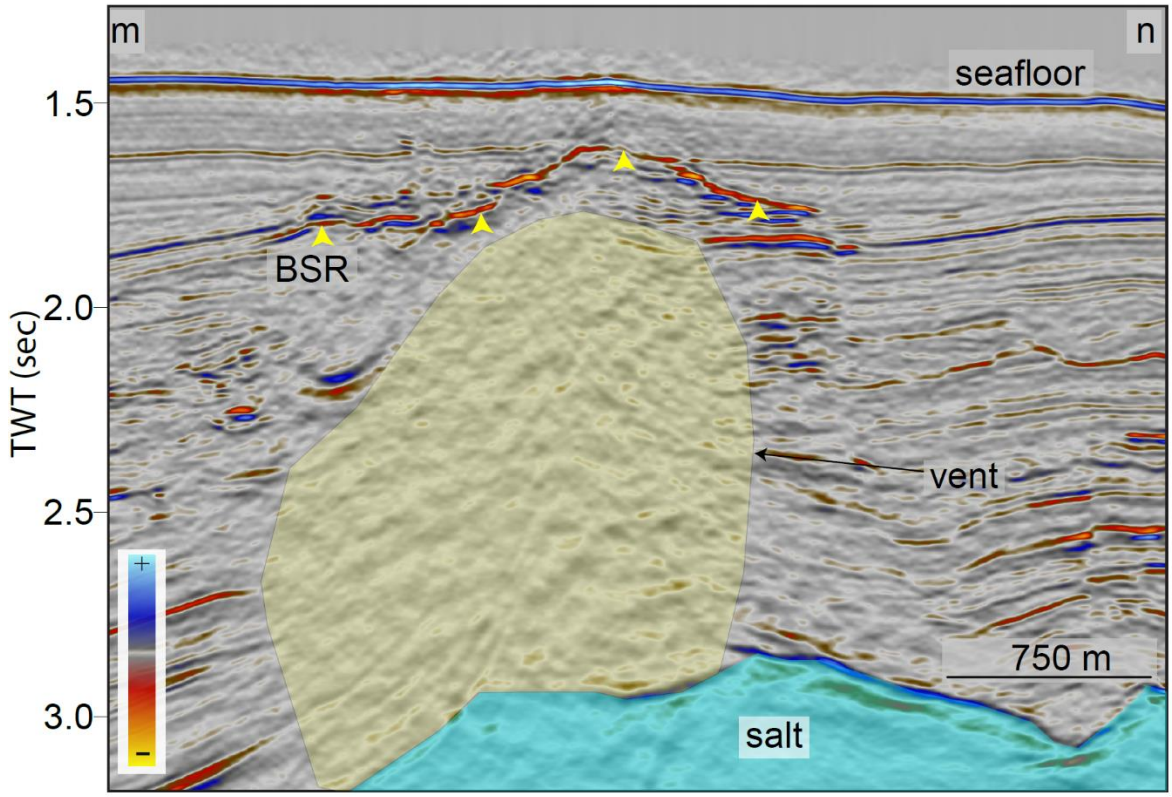


*Figure 21: Seismic profile m-n showing a west-east cross-section across the BSR system in Zone-4. The BSR is shown by the yellow arrows. The profile location is shown in Figure 20.*

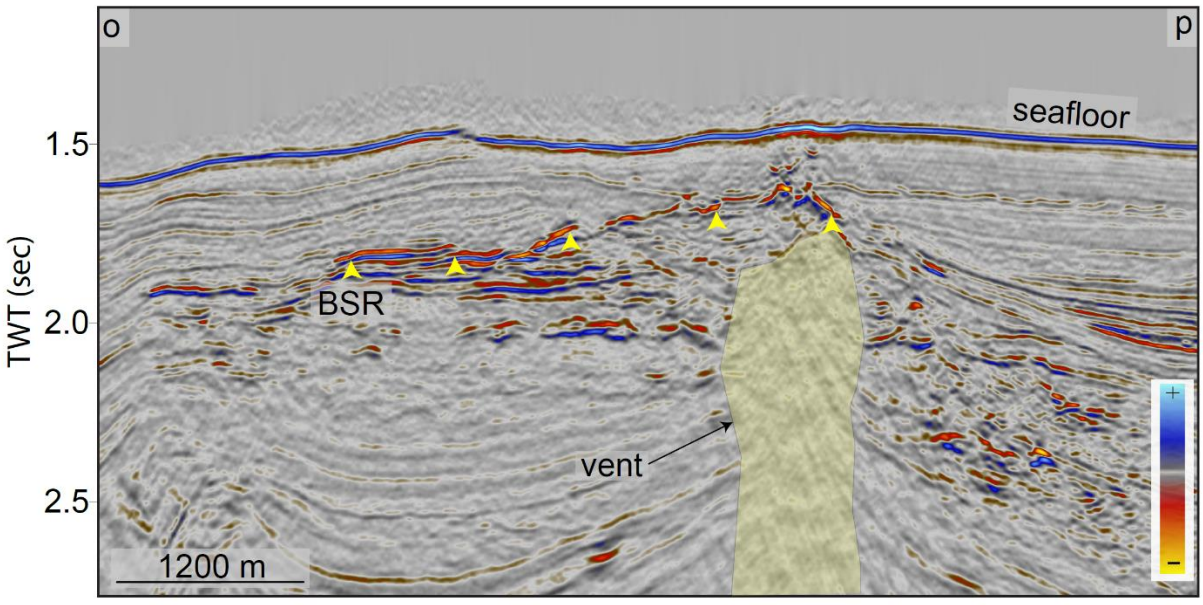


*Figure 22: Seismic profile o-p showing a south-north cross-section across the BSR system in Zone-4. The BSR is shown by the yellow arrows. The profile location is shown in Figure 20.*

# 5 Gas Resource Estimation

We calculate high and low estimates for the high-confidence gas hydrate accumulations based on the total area of possible peak-leading reflections above the BSRs. The low estimate is based on a 10 m-thick sand layer, 30% porosity, and 50% gas hydrate saturation. The high estimate assumes 30 m-thick sand layer, 40% porosity and 90% gas hydrate saturation. The Project Area 2.4 report provides details about the methodology and parameters used for resource estimation used in this report.

In Project Area 2.3, we map possible peak-leading reflections in Zone-1 (Figure 3) that occupy a total area of 0.35 $km^2$. Zones 2, 3, and 4 do not have peak-leading reflections and do not contribute to the resource estimation. Based on peak-leading reflections in Zone-1, minimum and maximum gas resource estimates are 0.1 and 0.6 billion cubic meters (BCM) or 3.53 and 21.18 billion cubic feet (bcf) respectively at STP (standard temperature and pressure).

# 6 Conclusion

In Project Area 2.3, we map six BSRs that span a total area of ~80 $km^2$. All mapped BSRs are associated with salt ridges and salt diapirs, like many other BSR's identified in Phase 1 and Phase 2 project areas in the northern Gulf of Mexico. The structural elements (faults and fractures) related to salt deformation likely act in some capacity to focus the gas to the overlying hydrate systems.

We mapped a possible peak-leading reflection in Zone-1, which covers a very small area of ~0.35 $km^2$. Considering only this possible peak-leading reflection, we estimate the volume of free gas at STP in this area of ~0.1 – 0.6 BCM (3.53 - 21.18 bcf). We characterize this estimate with low confidence as the presence and characterization of peak-leading reflection is strongly influenced by the data quality and signal frequency.

# 7 References


Cook, A., Sawyer, D., 2015. The mud-sand crossover on marine seismic data. Geophysics 80, A109–A114. https://doi.org/10.1190/GEO2015-0291.1

Hillman, J.I.T., Cook, A.E., Sawyer, D.E., Küçük, H.M., Goldberg, D.S., 2017. The character and amplitude of 'discontinuous' bottom-simulating reflections in marine seismic data. Earth Planet. Sci. Lett. 459, 157–169. https://doi.org/10.1016/j.epsl.2016.10.058

Kramer, K. V., Shedd, W.W., 2017. A 1.4-billion-pixel map of the Gulf of Mexico seafloor. Eos (United States). https://doi.org/10.1029/2017eo073557

Portnov, A., Cook, A.E., 2020. Gulf of Mexico Hydrate Mapping and Interpretation Analysis. Bureau of Ocean Energy and Management. Gulf of Mexico Hydrate Mapping and Interpretation Analysis (boem.gov)

Portnov, A., Cook, A.E., 2019. Gulf of Mexico Hydrate Mapping and Interpretation Analysis. Bureau of Ocean Energy and Management. Area-2-Results.pdf (boem.gov)

Portnov, A., Cook, A.E., Sawyer, D.E., Yang, C., Hillman, J.I.T., Waite, W.F., 2019. Clustered BSRs: Evidence for gas hydrate-bearing turbidite complexes in folded regions, example from the Perdido Fold Belt, northern Gulf of Mexico. Earth Planet. Sci. Lett. 528, 115843. https://doi.org/10.1016/j.epsl.2019.115843

Sassen, R., Losh, S.L., Cathles, L., Roberts, H.H., Whelan, J.K., Milkov, A. V., Sweet, S.T., DeFreitas, D.A., 2001. Massive vein-filling gas hydrate: Relation to ongoing gas migration from the deep subsurface in the Gulf of Mexico. Mar. Pet. Geol. 18, 551–560. https://doi.org/10.1016/S0264-8172(01)00014-9

Shedd, W., Boswell, R., Frye, M., Godfriaux, P., Kramer, K., 2012. Occurrence and nature of " bottom simulating reflectors" in the northern Gulf of Mexico. Mar. Pet. Geol. 34, 31–40. https://doi.org/10.1016/j.marpetgeo.2011.08.005

Skopec, S., Portnov, A., Cook, A.E., 2021. Gulf of Mexico Hydrate Mapping and Interpretation Analysis. Bureau of Ocean Energy and Management.

Triezenberg, P.J., Hart, P.E., Childs, J.R.C., 2016. National Archive of Marine Seismic Surveys (NAMSS): A USGS data website of marine seismic reflection data within the US Exclusive Economic Zone (EEZ)". US Geol. Surv. data release 10 F7930R7P. https://walrus.wr.usgs.gov/namss/search/

Vanneste, M., De Batist, M., Golmshtok, A., Kremlev, A., Versteeg, W., 2001. Multi-frequency seismic study of gas hydrate-bearing sediments in Lake Baikal, Siberia. Mar. Geol. 172, 1–21. https://doi.org/10.1016/S0025-3227(00)00117-1